РОССИЙСКАЯ АКАДЕМИЯ НАУК

Физический
институт
имени
П.Н.Лебедева

ФИАН

V.A. BASKOV, B. SHRODER,
B.B. GOVORKOV, A.I. LEBEDEV,
V.V. POLIANSKY

PREPRINT

5

THRESHOLD NEUTRAL PION PHOTOPRODUCTION IN HYDRODGEN AND DEUTERIUM

(PROJECT OF AN EXPERIMENT)

MOSCOW 2007

Threshold Neutral Pion Photoproduction in Hydrogen and Deuterium

(Project of an experiment)

V.A. Baskov, B. Shroder [a], B.B. Govorkov*, A.I. Lebedev, V.V. Poliansky

Abstract

In this work we propose two neutral pion photoproduction experiments near reaction threshold. Using lH_2 and lD_2 targets we can obtain the best world data for π^0-photoproduction. From these data we can extract the threshold E_{o+} $(\pi^0 n)$ amplitude for neutral pion photoproduction with high precision to test the self-consistency of Low Energy theorems (LET) for different channels of π^0-photoproduction and to test OCD-based theoretical predictions and, in particular, chiral perturbation theory (ChPT).

[a] - MAX-lab, Lund, Sweden
* - govorkov@x4u.lebedev.ru

> In any case, it would be very interesting to have an experimental determination of $\sigma_{tot}(\gamma n \to \pi^0 n)$ close to the threshold"
>
> V. Bernard, N. Kaiser, W. Meißner, Nucl, Phys.
> 383B (1992) 442–496.

1. Introduction

Recently investigations on pion photoproduction in nucleons have entered a new stage of their development. This is observed both in experiments and the theory and caused by the progress in the accelerators, the development of the γ-beam monochromatization technique and the development of detecting devices – e-, γ-, N-detectors etc. Such devices have been made as huge NaI(Tl) crystals having energy resolution $\Delta E_\gamma = (1–2)\%$, "walls" of GAMS γ-spectrometers, the development of TOF-technique etc.

As for the theory, the chiral perturbation theory have been developed that explains old problems of threshold pion photoproduction such as the unusual behavior of the energy dependence of the dipole amplitude $E_{o+}(\pi^0 n)$ in neutral pion photoproduction on protons near the threshold energy.

Now the experiments concerning pion photoproduction is preparing and carrying out in many scientific centers in a number of countries: MAMI at Mainz, Germany, GRAAL in Grenoble, Jefferson Laboratory in the United States, Laboratory on Osaka etc. We think that now the best place for pion photoproduction investigations near the threshold is Max-lab, Lund, Sweden.

Quantum chromodynamics gives sufficiently precise model-independent prediction for the threshold energies – Low Energy theorems (LET), so it is possible to verify this prediction in experiment.

When working with a hydrogen target, the following pion photoproduction processes take place in it:

$$\gamma + p = \underset{\hookrightarrow 2\gamma}{\pi^0} + p \qquad E_{th} = 144{,}68\ \text{MeV}, \qquad (1)$$

$$\gamma + p = \pi^+ + n \qquad E_{th} = 151{,}43\ \text{MeV}, \qquad (2)$$

When using a deuterium target the pion photoproduction processes are as follows:

$$\gamma + n = \underset{\hookrightarrow 2\gamma}{\pi^0} + n \qquad E_{th} = 144{,}67\ \text{MeV}, \qquad (3)$$

$\gamma + p = \pi^+ + n$ $E_{th} = 151{,}43$ MeV, (4)

$\gamma + n = \pi^- + p$ $E_{th} = 148{,}45$ MeV, (5)

$\gamma + p = \pi^0 + p$ $E_{th} = 144{,}68$ MeV, (6)
$\hookrightarrow 2\gamma$

$\gamma + d = \pi^0 + d$ $E_{th} = 139{,}833$ MeV, (7)
$\hookrightarrow 2\gamma$

When calculating threshold values we do not take into account the interaction of nucleons in a deuteron , but this can be easily done.

Each process occurring exactly at the threshold energy has only the S-wave dipole amplitude E_{0+}, therefore in this case the total cross section is equal to:

$$\sigma_{tot} = 4\pi \tfrac{q}{k} E_{0+}^2 \qquad (8)$$

Our aim is to determine the threshold value of E_{0+} ($\gamma n \to \pi^0 n$)-amplitude in experiment. There is a simple reason for this. Although the first determination of the value and the sign of the dipole amplitude E_{0+} ($\gamma p \to \pi^0 p$) = (-2.0 ± 0.2) $10^3/m_\pi$ was made 45 year ago, until now nobody determines the amplitude of photoproduction of neutral pions on neutrons E_{0+} ($\gamma n \to \pi^0 n$). There are many reasons for this:

- smallness of the cross section (about 0.1 μb or less);
- only neutral particles in the final state (n, γ);
- small angles of outgoing particles (exactly at the threshold the angle is 0°);
- gigantic electromagnetic background and background from photonuclear reactions.

Achievements of MAX-lab scientists and scientists from other laboratories (resolution of tagging systems ΔE_γ=0.2–0.3 MeV, accelerator and tagging systems rate 10^6 γ/Mev s, detecting devices) allow us to propose studying π^0 photoproduction in liquid-hydrogen and liquid-deuterium targets near the threshold energy E_γ = (130–200) MeV.

It is π^0 photoproduction in lH_2 and lD_2 that we propose to study in this Letter of Intent. In addition we may see the difference in π^0 photoproduction on free neutrons and neutrons bound in deuterium by detecting neutrons (angle and momentum measurements) from reactions (2) and (4). Simultaneous detection of neutrons from reactions (3) and (4) in identical kinematic regions may give the ratio of the S-wave amplitudes at the threshold. From LET we have:

$$\frac{E_{0+}(\gamma n \to \pi^0 n)}{E_{0+}(\gamma p \to \pi^+ n)} = \frac{K_n}{2\sqrt{2}} \frac{\mu^2}{(1 - \frac{3}{2}\mu)} \tag{9}$$

where K_n is the neutron anomalous magnetic moment, μ – the ratio of the pion and nuleon masses (m_π/m_N).

According to (9) the ratio of the total cross sections is:

$$\eta_{LET} = \frac{\sigma_{tot}(\gamma n \to \pi^0 n)}{\sigma_{tot}(\gamma p \to \pi^+ n)} = \frac{K_n^2}{8} \frac{\mu^4}{(1 - \frac{3}{2}\mu)^2} \cong 3 \cdot 10^{-4}$$

(10)

Channel	ChPT ($\times 10^{-3} m_\pi^{-1}$)	LET ($\times 10^{-3} m_\pi^{-1}$)	recent experimental value ($\times 10^{-3} m_\pi^{-1}$)
$\gamma + p \to n + \pi^+$	$+28.2 \pm 0.6$	$+27.6 \pm 0.2$	$+28.2 \pm 0.6$
$\gamma + n \to p + \pi^-$	-32.7 ± 0.6	31.7 ± 0.2	-31.5 ± 0.8
$\gamma + p \to n + \pi^0$	-1.16	-2.3	-1.32 ± 0.08
$\gamma + n \to n + \pi^0$	$+2.6$	-0.5	~ -0.4

The table above taken from the reference [2] shows that the ratio of cross sections for the reactions (3) and (4) is equal to $\eta_{LET} = 3 \cdot 10^{-4}$ according to LET, which emphasize difficulties of the measurements. True, if the ChPT is correct, the output of the π^0n-reaction will be 25 times higher ($\eta_{ChPT} = 25 \cdot \eta_{LET}$), which may be seen as the additional prove that the value of E_{0+} ($\gamma n \to \pi^0 n$) is very sensitive to fine QCD-effects such as $\pi^+ \to \pi^0$ recharging, the finiteness of quark masses in nucleons etc. It should be note that in the expansion of the E_{0+} ($\gamma n \to \pi^0 n$) amplitude in terms of μ the first non-zero terms are μ^2 terms, which explains sensitivity of this amplitude to such effects.

To bypass the difficulties mentioned above we propose – following Bergstrom et al [3] – to select the process $\gamma n \to \pi^0 n$ by registering the coincidence of the neutron (n) and one or two γ-quanta from the decay of the π^0-meson.

So, n + γ (2γ).

The study of the reaction $\gamma n \to \pi^0 n$ is carried out in the interval of 1 MeV for the incident γ-quanta above the threshold: $\Delta E_\gamma = [E_{th}; E_{th} + 1\text{ MeV}]$. To distinguish the processes $\gamma n \to \pi^0 n$ and $\gamma p \to \pi^+ n$ the difference of the threshold energies will be used: $\Delta E_{th} = 6.76$ MeV, which can be easily done with the MAX-lab accelerator and tagging systems.

The proposed task is the most beautiful, but also the most difficult one in pion photoproduction. To detect neutrons we propose to use a wall of ring neutron detectors located in the forward direction concentrically relative to the direction of the incident beam of tagged γ-quanta. To detect γ-quanta from the π^0-decay a "sandwich" with high geometrical effectiveness will be used. We need to detect only the fact of appearing a high-energy γ (for suppressing of the background processes). The neutron- and γ-detectors is described further in this Letter of Intent.

When measuring the threshold value of E_{o+} $(\pi^0 n)$ the problem is reduced to determining the value of the initial energy of the tagged photons as near as possible to the threshold energy E_{th} (144,67 MeV). It requires that the tagged photon systems have very high energy resolution near the threshold: $\Delta E_\gamma \approx 0.2$ MeV. The MAX-lab system consisting of the accelerator and the tagging system is ideally suited for such measurements. In this case the value σ_{tot} $(\gamma n \rightarrow \pi^0 n)$ will be measured. Now there are no other places in the world where the fundamental process $\gamma + n \rightarrow \pi^{0+} n$ at the threshold energy could be measured.

2. The kinematics of the processes

First consider the kinematics of neutrons near the threshold. All neutrons created in the process $\gamma + n \rightarrow \pi^0 + n$ at the threshold energy is known to move exactly in the direction of the incident photons and have the energy E_{neutr}=8,475 MeV. The photon energy increasing, the range of outlet angles widens and correspondingly the range of neutron energies widens too. Fig 1 shows the neutron energy E_n versus the outlet angle Θ_n for two reactions $\gamma n \rightarrow \pi^0 n$ and $\gamma p \rightarrow \pi^+ n$ and four (five) energies of incident photons.

We see from this figure that the curves for the two processes are practically identical and each curve can be obtained from the other one by an appropriate shift along the energy axis. Therefore when detecting neutrons in an energy interval $[E_\gamma; E_{th} - E_\gamma]$ the curves for the interval 1 MeV under the kinematics threshold are indentical, but the interval is E_γ=[144.67; 145.67] MeV for the $\pi^+ n$-process and E_γ=[151.43; 152.43] MeV for the $\pi^0 n$-process.

In both cases the range of outlet angles of neutrons is 1–6°. Naturally measurements for both processes being studied is carried out simultaneously in the same "run".

The table below illustrates the features of neutrons and pions in the processes being investigated. The table shows kinematics values for the interaction of a photon with the energy 144.94 MeV and a neutron at rest (without taking into account the binding energy in deuterium). Fig. 2 shows the angles of outgoing neutrons versus the angles of pions at various energies of the incident photons. Complex kinematical interconnections are seen in the interval (1–1.5) MeV above the threshold, and it should to be very careful when making measurements in these intervals. It should be noted that the pion momentum rapidly increases in this 1-MeV interval and, considering the strong dependence of the measured cross sections on the energy, this leads to difficulties in measuring such cross sections in the threshold region of energies. It should be stressed that the measurement of σ_{tot} $(\gamma n \rightarrow \pi^0 n)$ in the 1 MeV interval above the threshold is a worthy and solvable problem for the MAX-lab. At the first stage the measurements can be limited to relative measurements by comparison of the total cross sections σ_{tot} ($\gamma n \to \pi^0 n$) and σ_{tot} ($\gamma p \to \pi^+ n$) obtained in the same experiment for the same areas on the (E_n; Θ_n) plane (see Fig. 1) and excluding the influence of bindness and by comparison of σ_{tot} ($\gamma p \to \pi^+ n$) on free neutrons (hydrogen) and bound neutrons (deuterium).

$E_\gamma = 144.94$ MeV max angle 3.375°

Θ_n	0°		1°		2°		3°	
E_n^{kin} (+) and (–) solutions, MeV	9.537	7.5322	9.4862	7.5725	9.3179	7.7092	8.9386	8.0363
E_n, MeV	949.099	947.098	949.0518	947.1381	948.8835	947.2748	948.504	947.602
p_n, MeV	134.1865	119.2089	133.4759	119.5285	132.6516	120.6072	129.9106	123.150
β_n	0.4266	2.4314	0.4776	2.3911	0.6457	2.2616	1.0246	1.9276
E_π^{kin} (+) and (–) for n, MeV	0.14138	0.125868	0.140641	0.12620	0.13980	0.12732	0.13696	0.12996
E_π, MeV	135.403	137.4078	135.454	137.3675	135.6221	137.2308	136.001	136.904
p_π, MeV	10.7398	25.7347	11.3624	25.5187	13.2184	24.7722	16.666	22.891
β_π	0.079317	0.18729	0.08388	0.1857695	0.097465	0.18051	0.12254	0.16720
Θ_π	0	0	11.8305	4.6889	20.500	9.78259	24.07675	16.3533

In table: E_n^{kin} (E_π^{kin}) - kinetic energy n (π); E_n (E_π) – energy n (π); p_n (p_π) – impulse n (π); (β_n) (β_π) - relative speed v_n/c (v_π/c); Θ_n (Θ_π) - outgoing angle n (π).

To suppress the background (electromagnetic etc.) we propose to use a lead-scintillator "sandwich" with high geometrical effectiveness close to 4π. The sandwich will detect photons from the decay of π^0 arising in the target (1γ- and 2γ-methods are possible depending on the background intensity). Thus we propose to detect the neutron (momentum, outgoing angle) and γ (or 2 γ) for the reaction $\gamma n \to \underset{\hookrightarrow 2\gamma}{\pi^0} n$. We need only to determine the presence of a high energy photon or two coinciding photons.

3. Experimental set-up for studying π^0 photoproduction on neutron near the threshold

The experimental set-up designed for studying threshold π^0 photoproduction consists of a lead-scintillator 4π-detector for π^0 registration and a neutron spectrometer (Fig. 3).

Neutron spectrometer

The main purpose of the neutron spectrometer is detecting neutron, determining its energy and its angle of departure from the target.

The time-of-flight (TOF) method will be used for determining the neutron momentum. A signal from the tagging system and signals from the γ-counters of the

4π-detector will be used as the start signal, while a signal from the neutron spectrometer will be used as a stop signal. The number of the fired element of the neutron detector indicates the angle of departure.

The neutron spectrometer consists of 5 rings made of plastic scintillator (Fig. 4). The thickness of each ring along the beam is 50 mm. The kinematic calculations show that the working position of the neutron detector corresponds to the distance from the target S = 260 cm. The dimensions of the rings, their azimuth angles of detection and their angular widths are shown in the Table 1.

Dimensions of the rings and overlapping angles of the neutron spectrometer

Ring number	Inner radius (R_{in}), mm	Outer radius (R_{out}), mm	Azimuth angle (θ), °	Angular width of the ring (Δθ), °
1	47	82	1.421	0.771
2	87	122	2.302	0.770
3	127	162	3.181	0.769
4	167	202	4.059	0.767
5	207	242	4.935	0.765

The part of the γ-beam that does not interact in the target goes through the center of the smallest ring. In order to collect light from particles going through the scintillators more effectively each ring of the neutron spectrometer is divided in two halves along its diameter. The light is taken from the end-surfaces of these half-rings with photomultipliers. All planes and end-surfaces of the rings have been polished. Each half-ring is wraped with metallized Mylar and covered with light-absorbing black paper.

The half-rings along with the PMTs and dividers from the first and second part of the rings are arranged on two plates of rigid foamed plastic. We use foamed plastic to reduce background interactions of the γ-beam with spectrometer parts. Both foamed plastic plates are inserted in a metal frame in such a way that the spectrometer is seen as five independent rings from the direction of the γ-beam. The total dimensions of the neutron spectrometer are $800\times 130 \times 153$ mm^3.

The time-of-flight method and the parameters of the neutron spectrometer were chosen on the basis of analysis for the angles of the neutron to be detected in the appropriate reactions. The range of neutron energies to be detected is E_n = 7–11 MeV. At a time-of-flight base of S = 2600 mm (Fig. 1) the time of flight is

T = 71.466 ns for E_n = 7 MeV

T = 57.191 ns for E_n = 11 MeV.

So the range of times to be detected is 55–75 ns. If the base S has some different value the time-of-flight interval shifts. The neutron energy is measured with the following accuracy:

$$\Delta E_n\ (\mathrm{MeV}) = E_n \cdot (pc/m_0c^2)^2 \cdot ((\Delta S/S)^2 + (\Delta T/T)^2)^{1/2},$$

where p – the neutron momentum; c – the speed of light; m_0 – the neutron mass; S – the base; ΔS – the variation of the base (the ring thickness); T – the time of flight for a neutron with an appropriate energy; ΔT – the accuracy of time of flight measurements.

When the base and the ring thickness is given, ΔE_n is determined by ΔT. Let $\Delta S/S=\Delta T/T$ then at $\Delta S= \pm 25$ mm (the thickness of the rings) the accuracy inmeasurements of the time of flight will be

$\Delta T = 0.687$ ns for $E_n = 7$ MeV

$\Delta T = 0.550$ ns for $E_n = 11$ MeV.

Considering finite dimensions of the target (50–70 mm) the accuracy should be 1.41 times higher. So the required accuracy of the neutron spectrometer is $\Delta T = 0.8$–1 ns.

The chosen base of 2600 mm and the estimated divergence of the γ-beam prevent the spectrometer from overloading. However when the background intensity increasing it is possible to reduce it by separating the rings from each other, but it is necessary to consider the changed configuration of the neutron spectrometer after this operation.

To suppress the background of low-energy charged particles arising in electromagnetic processes an anticoincidence counter ($20\times500\times500$ mm^3) is placed in front of the neutron spectrometer.

A sectioned lead-scintillator spectrometer (with internal trigger) located in the backward hemisphere of the set-up will be used as the monitor (Fig. 3).

Lead-scintillator 4π-detector

The neutral pions arising in interactions of tagged photons with the target are detected by a 4π-detector, consisting of a set of 6 independent detectors. The detector registers secondary γ-quants from the pion decay. The tagged photon energy and the neutron energy determine the pion energy in the region near the threshold. The main task of this detector is to confirm the fact of presence of π^0 in the reaction.

The lead-scintillator 4π-detector (Fig. 5) consists of 6 trapezoidal sections. The cross section of the spectrometer has a hexagonal form with the described circle radius 35 cm. The central hole of the spectrometer where the target is located also has a hexagonal form with the described circle radius 8 cm. Each section represents a lead-scintillator assembly of the "sandwich" type that consists of a set of lead plates 3 mm width and plastic scintillators.

The left and right sections relative to the incident γ-beam consist of 4 scintillator plates 50 mm width that are sandwiched with 4 lead plates. The two upper and two lower sections consist of 5 scintillator plates 40 mm width that are sandwiched with 5 lead plates. For all sections the dimensions of the facet nearest to the beam are 70x500 mm^2, while the dimensions the farthest facet are 300x500 mm^2. Scintillators and photomultipliers of each section of the 4π-detector are placed into a metal casing with the total length 1755 mm.

The light produced in each section of the detector is taken from the both end-surfaces of the lead-scintillator assembly through an air gap (using a reflecting cone of metallized Mylar) with photomultipliers.

The trigger indicating a possible pion decay is a coincidence of signals from two opposite sections as well as a signal from one of the 6 sections.

Time resolution of the spectrometer is about 15 ns. Although γ-quanta do not leave all their energy in the detector, each section and the whole detector have spectrometric properties. If the energy of γ is 30–80 MeV and the detecting effectiveness is 85%, the energy resolution of a section is 45%. If the energy of γ is 80–170 MeV and the detecting effectiveness is more than 90%, the resolution is about 30%. Thus the 4π-detector along with the tagging system can determine the pion energy with 90% effectiveness but with much worse accuracy.

To exclude the background of low-energy charged particles relating to electromagnetic interactions 6 thin anticoincidence scintillator detectors (10×70×500 mm^3) will be placed between the target and each section of the 4π-detector.

This fast 4π-detector belongs to so-called self-triggered detectors or detectors that can form their own trigger.

4. Reaction output – number of detected events

The trigger for the reaction $\gamma+n\to\underset{\hookrightarrow\gamma+\gamma}{\pi^0}+n$

is the coincidence of one or two γ-quanta from the decay of π^0 and a tagged photon γ_{tag}.

The output of the reaction will be

$$Y = \Pi\cdot\sigma\cdot N\cdot\varepsilon_n\cdot\varepsilon_\gamma\cdot\varepsilon_{tag},$$

where Π – flux of tagged γ in the 1 MeV interval above the threshold;
σ – total cross section of the processes being studied;
N – number of neutrons in the deuterium target;
ε_i – detecting effectivenesses for neutrons, γ from the π^0 decay and tagged γ in the 1 MeV interval.

If we have the following conditions for a MAX-lab tagging system:
lD_2 target is 10 cm along the beam of γ_{tag} or $N = 10^{24}$;
$\Pi = 10^6$ γ/s MeV;

$\sigma(\gamma p \to \pi^+ n) \approx 12\ \mu b$;
$\sigma(LET) = \sigma(\gamma n \to \pi^0 n) = \eta_{LET} \cdot \sigma(\gamma p \to \pi^+ n) = 3\cdot 10^{-4} \cdot 12 = 3.6 \cdot 10^{-3} \approx 4 \cdot 10^{-3}\ \mu b$;
$\sigma(ChPT) = \sigma(\gamma n \to \pi^0 n) = \eta_{ChPT} \cdot \sigma(\gamma p \to \pi^+ n) = 3\cdot 10^{-4} \cdot 25 \cdot 12 = 9 \cdot 10^{-2} \approx 0.1\ \mu b$;
$\varepsilon_n\ \varepsilon_\gamma\ \varepsilon_{\gamma tag} = 0.2 \cdot 0.9 \cdot 1.0 \approx 0.2$;
$Y(LET) = 10^6 \cdot 4\cdot 10^{-33} \cdot 10^{24} \cdot 0.2 = 8 \cdot 10^{-4}$ 1/s;
$Y(ChPT) = 10^6 \cdot 0.1\cdot 10^{-30} \cdot 10^{24} \cdot 0.2 = 2 \cdot 10^{-2}$ 1/s;
we obtain $36\cdot 10^3$ events in case of ChPT correctness and $14.4\cdot 10^2$ events in case of LET correctness for 500 hours. If we divide the 1 MeV interval into 5 equal bins 0.2 MeV each, then we will have $7{,}2\cdot 10^3$ events and $2{,}88\cdot 10^2$ events per bin correspondingly, or the statistical accuracy will be 1.2% and about 6% correspondingly. The exact geometry and amount of statistics will be clear after simulation with the GEANT program.

So to solve the fundamental problem of measuring E_{0+} $(\pi^0 n)$-amplitude we need 500 working hours of the MAX-lab accelerator in case of the deuterium target and about 200 working hours in case of hydrogen target.

In conclusion it should be noted that as a by-product we detect 1.2 10^6 events of the reaction $\gamma + p \to n + \pi^0$ for the same 500 working hours, which can be also used for substantial checking of LET.

Note that if our methods of distinguishing investigated reaction turn out insufficient, the method of discriminating n and γ according to the pulse form from the detected neutrons may be added.

References

1. Goldansky V.I., Govorkov B.B., Vassilkow K. G. Nucl. Phys, **12** (1959) 327–332;
   Baldin A.M., Govorkov B.B.Doklady Akademii Nauk, **127** (1959) 993–996 (in Russian).
2. Fissum K., O'Reilly G. A letter of intent to the MAX-lab PAC, submitted 2 May 2002.
3. Bergstrom J. C. et al. Phys. Rev. C, **55** (1997) 2923-2930.

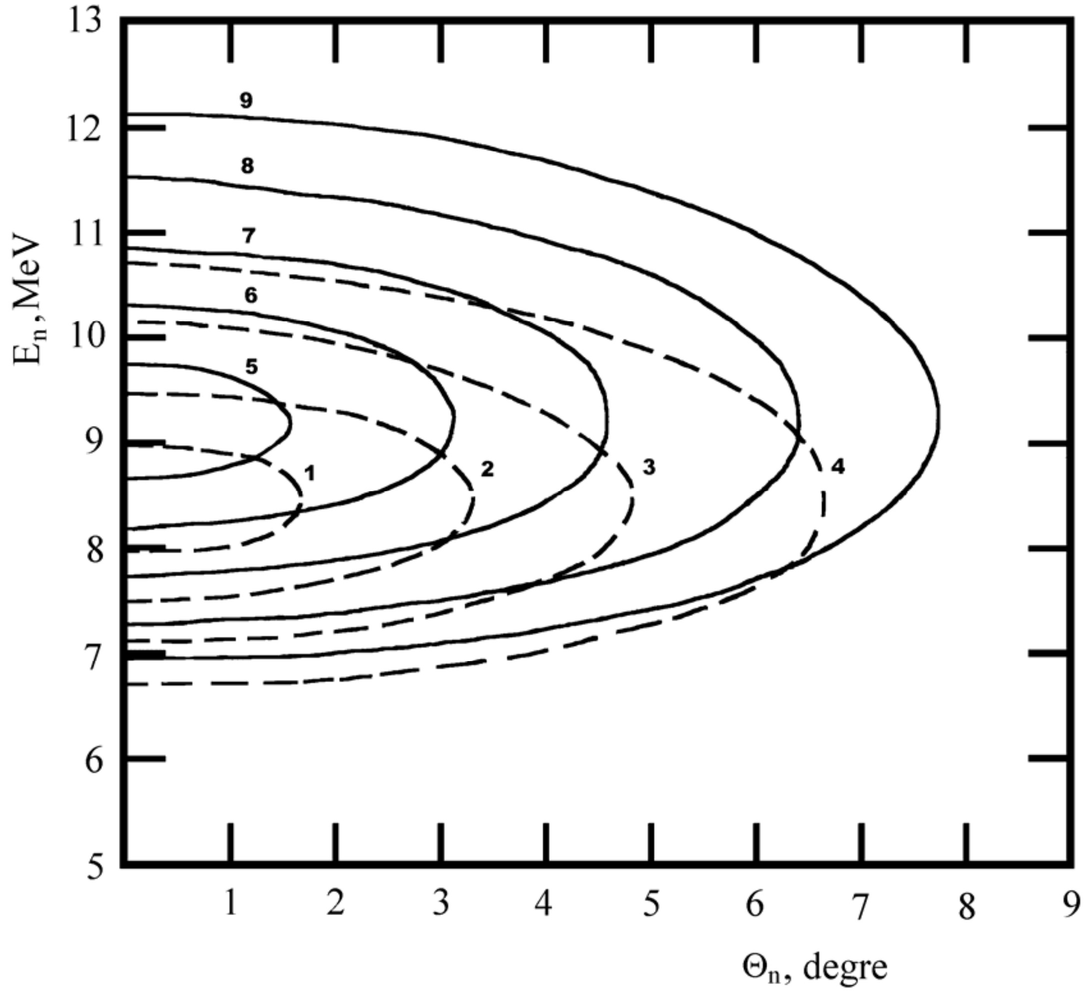

Fig. 1 The neutron energy E_n versus the outlet angle Θ_n for two reactions $\gamma n \rightarrow \pi^0 n$ and $\gamma p \rightarrow \pi^+ n$ and four (five) energies of incident photons.

$\gamma n \rightarrow \pi^0 n$	$\gamma p \rightarrow \pi^+ n$
1 – E_γ = 144,74 MeV	5 – E_γ = 151,5 MeV
2 – E_γ = 144,94 MeV	6 – E_γ = 151,7 MeV
3 – E_γ = 145,24 MeV	7 – E_γ = 152,0 MeV
4 – E_γ = 145,74 MeV	8 – E_γ = 152,5 MeV
	9 – E_γ = 153,0 MeV
	($E_\gamma^{threshold}$ = 151,43 MeV)

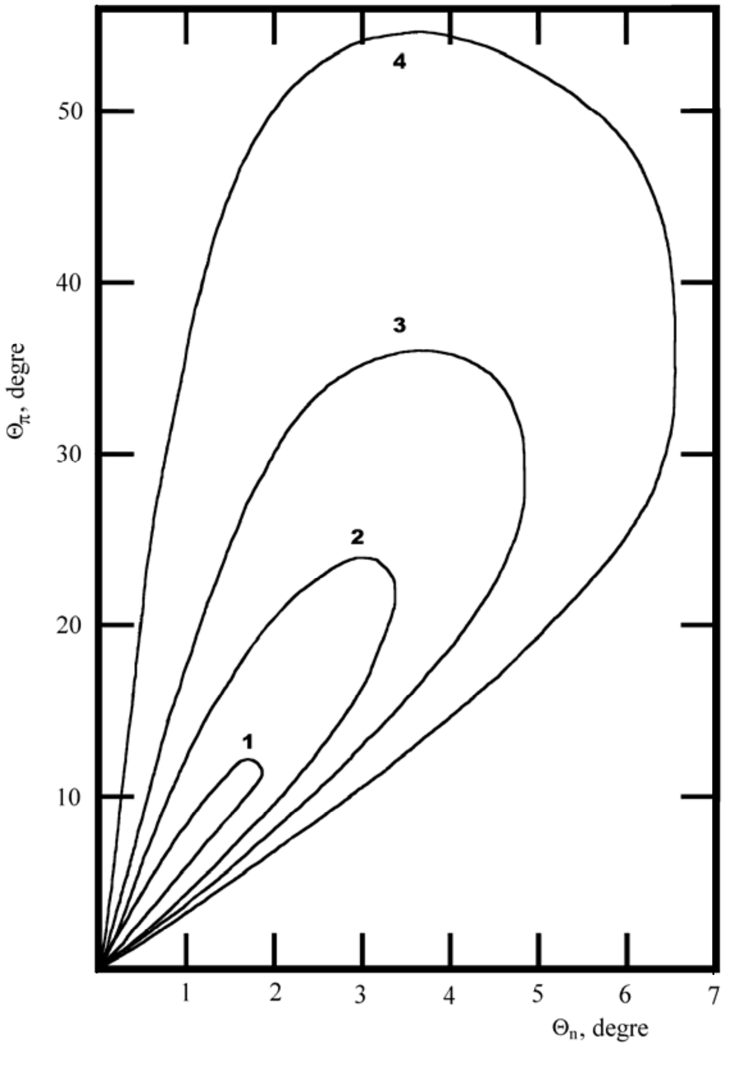

Fig. 2 The angles of outgoing neutrons (Θ_n) versus the angles of pions (Θ_π) at various energies of the incident photons.
1 – E_γ = 144,74 MeV; 2 – E_γ = 144,94 Mev; 3 – E_γ = 145,24 MeV; 4– E_γ =145,74 MeV.

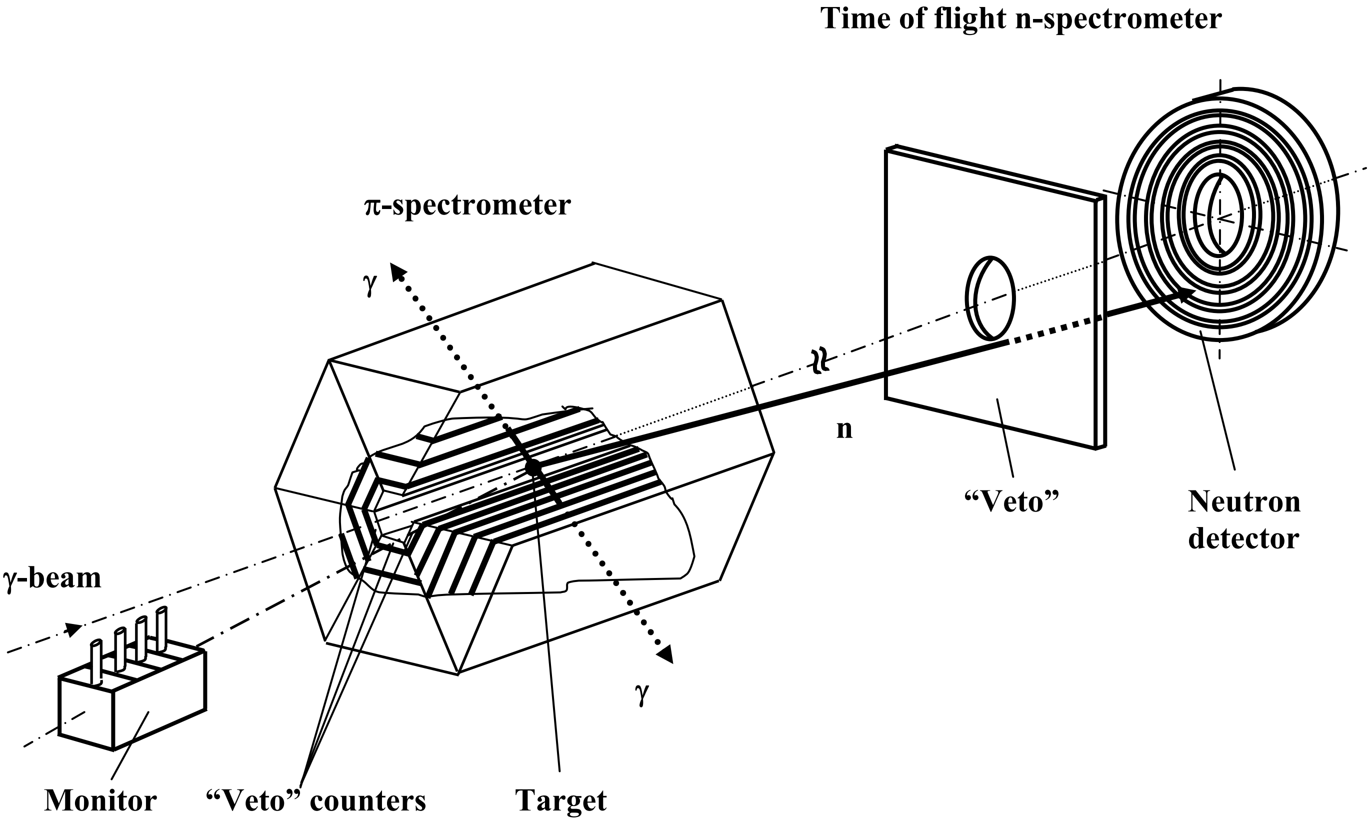

Fig. 3. The experimental set-up.
In the π-spectrometer one scintillation section is absent.

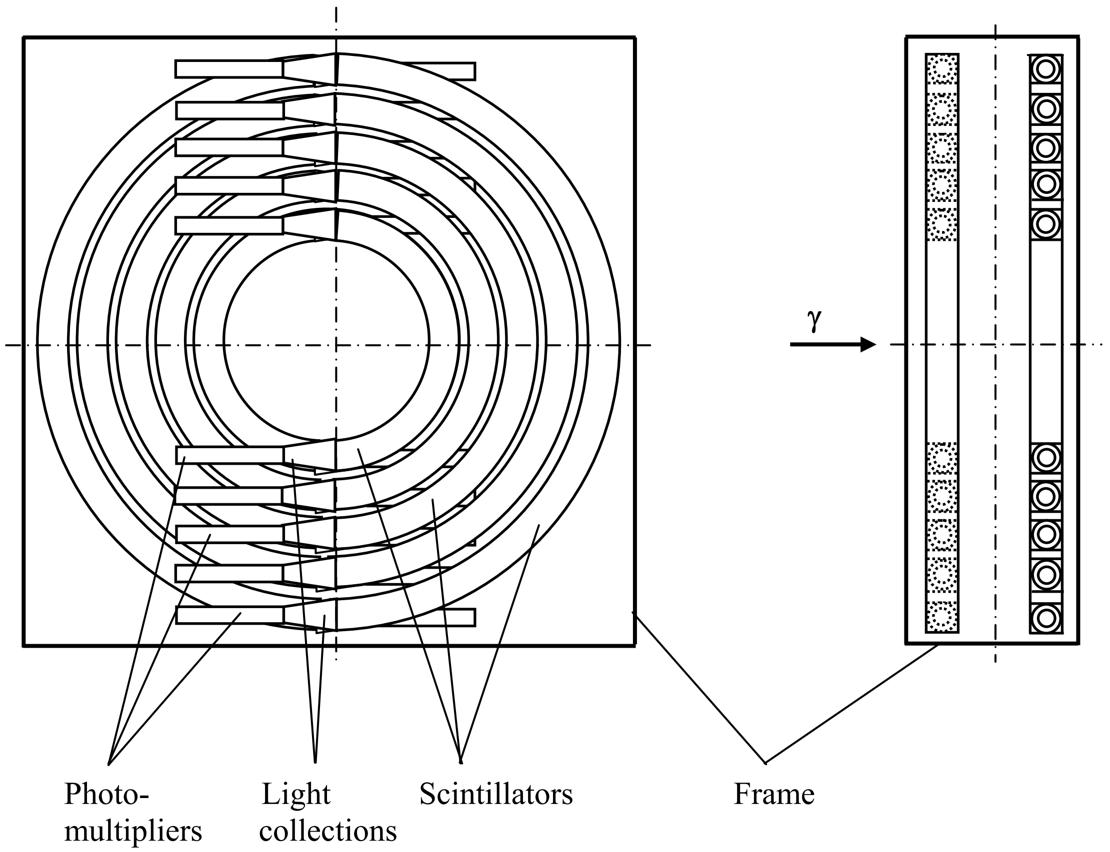

Fig. 4 Common view of n-spectrometer.

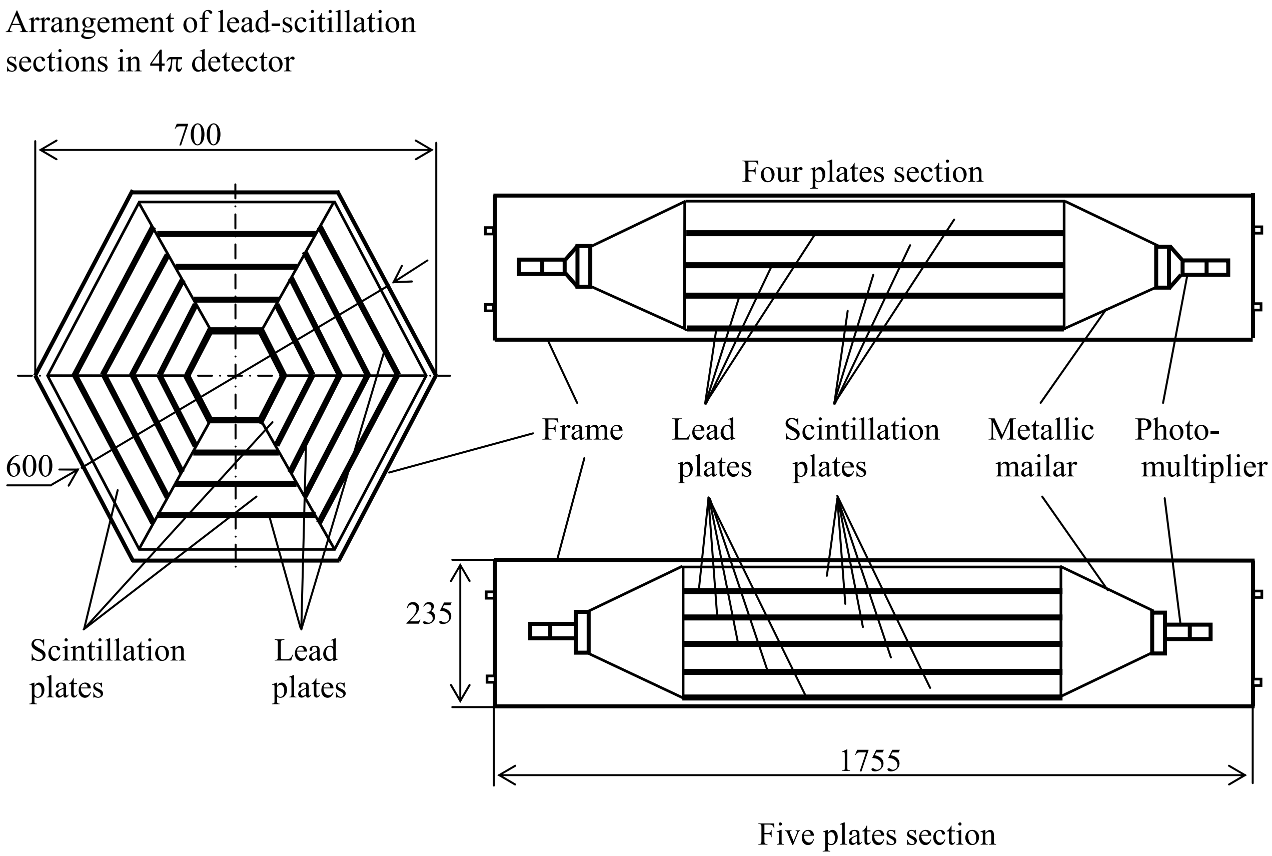
Arrangement of lead-scitillation sections in 4π detector

Four plates section

Five plates section

Fig. 5 Scheme of 4π detector.